ChemComm

Accepted Manuscript

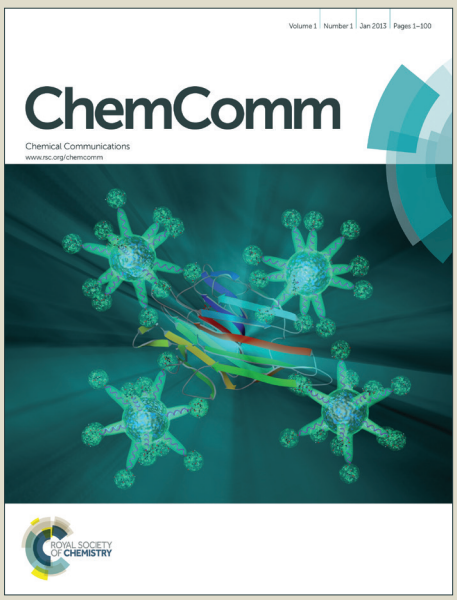

ROYAL SOCIETY OF CHEMISTRY

www.rsc.org/chemcomm

Journal Name

COMMUNICATION

Gold-Installed Biostable Nanocomplexes for Tumor-Targeted siRNA Delivery *In Vivo*

Received 00th January 20xx,
Accepted 00th January 20xx

DOI: 10.1039/x0xx00000x

www.rsc.org/

Roun Heo,[a] Hong Yeol Yoon,[b] Hyewon Ko,[a] Jung Min Shin,[b] Jueun Jeon,[b] Yee Soo Chae,[c] Young Mo Kang,[c] Dukjoon Kim,[b] Doo Sung Lee[b] and Jae Hyung Park[*ab]

The key issues, associated with nanocarriers for small interfering RNAs (siRNAs), are their poor stability and lack of tumor targetability *in vivo*. To address these needs, we developed gold-installed polyethyleneimine/siRNA complexes with a corona of PEGylated hyaluronic acid.

RNA interference (RNAi) has emerged as a powerful genetic approach for efficiently silencing target genes and regulating levels of endogenous proteins.[1-3] It is being harnessed to silence mRNAs encoding pathogenic proteins for the treatment of several diseases, including muscular degeneration, diabetes, and cancer.[4, 5] Among the various types of RNAi-based therapeutics, small interfering RNA (siRNA) is a potential next-generation medical breakthrough, since it has superior gene silencing effects and has no side effects compared to conventional antisense oligonucleotides.[6] In order for siRNA to have therapeutic efficacy, it should be delivered to the cytosol after being taken up by the target cell. Meanwhile, siRNAs are easily degraded by enzymes and their negatively charged surface prevents their internalization into cells.[7] Also, siRNAs are not cell specific as they are not targetable. To overcome these problems and enhance the therapeutic efficacy of siRNAs, novel carrier systems that can improve the stability of siRNAs and deliver them to specific target cells are needed. So far, various carrier systems have been developed including viral and non-viral vectors.[5, 8, 9] Since viral vectors can potentially induce immune and toxic reactions, development of non-viral vectors has been actively pursued. Nonetheless, clinical applications of non-viral siRNA delivery systems have been limited because their vulnerable structure, mainly based on electrostatic interactions, can easily dissociate and release siRNA before reaching the target site *in vivo*. The prematurely released siRNA could rapidly degrade into ineffective fragments in the RNase-rich physiological environment, resulting in poor therapeutic efficacy. Recently, a few attempts have been made to improve the stability of the siRNAs by layer-by-layer coatings, their conjugation to polymers, and chemical crosslinking of complexes.[10-13] Nevertheless, most non-viral vector systems have not exhibited the effective gene silencing efficacy *in vivo* because they do not possess tumor targetability.

Gold nanoparticles (AuNPs) have received increasing attention for biomedical applications, primarily ascribed to their excellent biocompatibility and facile modification.[14, 15] For siRNA delivery, AuNPs have been often used as the substrates for conjugation of siRNA.[16] For example, Giljohann et al. developed a polyvalent siRNA-nanoparticle conjugation method to attach siRNAs onto the surface of AuNPs via a thiol group, leading to prolonged siRNA circulation time in the blood.[11]

Hyaluronic acid (HA), a natural polysaccharide found in the extracellular matrix of the body, plays important roles in cell adhesion, proliferation and differentiation.[17, 18] In recent years, HA is emerging as a drug and gene carrier because it is biodegradable and can bind to CD44, which is over-expressed in cancer cells.[19, 20] Notably, HA-based nanoparticles are useful for intracellular delivery of the payloads because HA is readily degraded by hyaluronidase-1 (Hyal-1), abundant in various malignant tumors.[21] However, the systemic administration of HA has led to its major accumulation in liver which has the other receptor for HA, referred to as HARE.[22] Previously, we demonstrated that conjugation of polyethylene glycol (PEG) at the backbone of HA can dramatically reduce liver-specific accumulation without significant deterioration of tumor targetability.[23, 24]

In an attempt to establish a siRNA carrier system with high stability and tumor targetability, we herein developed gold-installed polyethyleneimine (PEI)/siRNA complexes with a corona of PEGylated HA (GICs). It was hypothesized that, as shown in Fig. 1, the unique structure of GICs would provide advantages for siRNA delivery: i) AuNPs, grown on the PEI/siRNA complexes, enhances the stability of GICs, ii) The corona of PEGylated HA increases possibility of GICs to reach the tumor site after systemic administration, iii) Upon

[a] *Department of Health Science and Technology, SAIHST, Sungkyunkwan University, Suwon 440-746, Republic of Korea. Tel: +82-31-290-7288; fax: +82-31-292-8790; e-mail: jhpark1@skku.edu.*
[b] *School of Chemical Engineering, Sungkyunkwan University, Suwon 440-746, Republic of Korea.*
[c] *School of Medicine, Kyungpook National University, Daegu 702-701, Republic of Korea.*

†Electronic Supplementary Information (ESI) available: Experimental details, Fig. S1-S4, and Table S1. See DOI: 10.1039/x0xx00000x

internalization of GICs in cancer cells, the nanostructure of GICs is loosen because Hyal-1 and glutathione (GSH) in the intracellular compartments may cause degradation of HA and dissociation of AuNPs from the complexes, respectively, and iv) siRNA can be effectively released by the proton sponge effect of PEI.

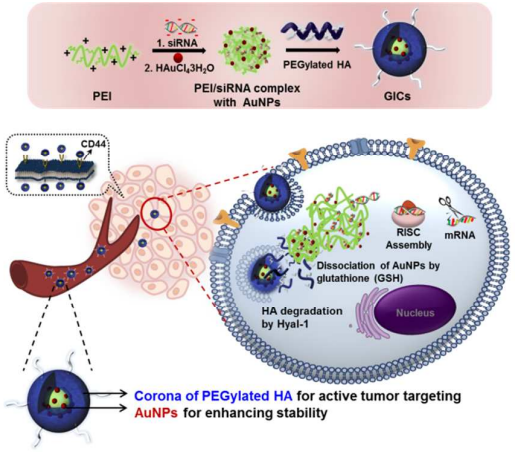

Fig. 1 Schematic illustration of GICs for cancer cell-specific siRNA delivery.

In order to verify the hypothesis, the stability and gene silencing efficiency of GICs were evaluated in the presence of serum and compared to the stabilities and efficiencies of free siRNA and gold-deficient PEI/siRNA complexes with a corona of PEGylated HA (GDCs). To assess *in vivo* biodistribution and tumor targetability, cyanine 5.5 (Cy5.5, a fluorescent dye)-labeled complexes were visualized using a non-invasive near-infrared fluorescence (NIRF) imaging system after systemic administration in tumor-bearing mice. Finally, using a red fluorescence protein (RFP)-B16F10 tumor-bearing mouse model, the *in vivo* gene silencing efficacy of GICs was evaluated.

In order to obtain GICs, gold was installed by growing AuNPs through reduction of $HAuCl_4$ on the PEI/siRNA complexes, followed by surface coating with PEGylated HA (Fig. 1). The complex formation was evaluated using a gel retardation assay by varying the weight ratio of PEI to siRNA ranging from 0.5:1 to 2:1 (Fig. S1b). The PEI/siRNA complexes showed siRNA retardation by the ratio of 0.8:1. AuNPs have been prepared by reducing $HAuCl_4$ in the presence of amine, as described elsewhere.[25-27] Therefore, it can be expected that PEI allows for formation of AuNPs on the complexes. Interestingly, for the complex with a ratio of 0.8:1, no retardation of siRNA was observed after growth of AuNPs. This implies that gold installation plays a valuable role in the stability of the complexes. The formation of AuNPs was also confirmed by UV-vis spectroscopy and TEM image (Fig. S1c). The UV-vis spectra showed a plasmon band at 525 nm, evidencing the existence of AuNPs. The TEM images revealed that the complexes were decorated with AuNPs (~10 nm in diameter) on their surfaces. Although the complexes are not fully covered by AuNPs, their growth is involved in multiple PEI chains. Therefore, it is expected that AuNPs can play a role as the crosslinker, which may improve the stability of complexes. To obtain insight into complexes under the physiological condition, gel retardation assays were also performed in the presence of heparin or heparin combined with GSH (Fig. S1b). Since heparin is a negatively charged polysaccharide in the body, it has an ability to dissociate the complexes.[28] On the other hand, GSH would displace the AuNPs from the complexes because it can acts as a strong competition molecule.[29] In the case of complexes without AuNPs, free siRNA bands were clearly visible in both the heparin and heparin with GSH-treated conditions. By contrast, free siRNA bands were only observed when GSH was used to treat the complexes with AuNPs. These results suggest that gold-installed complexes would remain unscathed in the bloodstream and be able to release siRNA efficiently at the intracellular level when exposed to GSH which is abundant in intracellular environments.

The physicochemical characteristics of complexes including surface functionality, size and charge have significant biological implications for their fates *in vivo*.[30] For this reason, we carefully investigated the properties of complexes at each step of our process. As shown in Table S1, the hydrodynamic size of PEI/siRNA complexes, GDCs, and GICs gradually increased with a mean diameter of 213.0 ± 5.56, 247.6 ± 1.63 and 327.6 ± 10.24, respectively. This implies that the hydrophilic PEGylated HA increased the size of both GDCs and GICs. Since GICs have AuNPs decorating their surfaces, they are larger in size than GDCs. The zeta potential values of PEI/siRNA complexes, GDCs and GICs were 44.4 ± 2.46, -5.58 ± 0.18 and -7.58 ± 0.81, respectively, indicating that GDCs and GICs were efficiently coated with PEGylated HA. The TEM images confirm the formation of complexes with a spherical morphology (Fig. S1d). In subsequent experiments, complexes with a 0.8:1 weight ratio were used as representative samples.

To evaluate the stability of the complexes under physiological conditions, the free siRNA, GDCs and GICs were incubated in the presence of 50% rat serum. The siRNA band intensities were examined at different time intervals via the gel retardation assay. As shown in Fig. 2a, for free siRNA and GDCs, the siRNA bands were dramatically decreased after 1 h and 3 h incubation, respectively. On the other hand, GICs consistently retained the structural integrity of the siRNA for up to 24 h. In contrast, free siRNA was completely degraded after 12 h. This tendency is apparent in the quantitative analysis graph constructed by measuring the intensity of each band (Fig. 2b). Surprisingly, GICs showed no significant decrease in the intensity of bands over the entire period of time tested, such that almost 100% of the siRNA was preserved after 24 h. These results suggest that AuNPs improved the stability of complexes in the presence of serum, thereby maintaining the structural integrity of siRNA for extended periods of time.

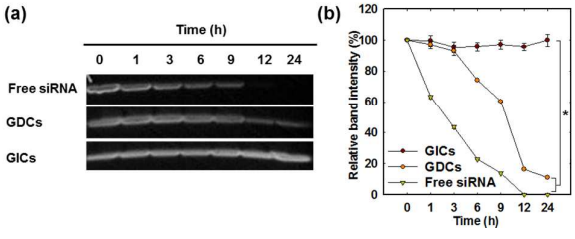

Fig. 2 Stability of free siRNA, GDCs and GICs in serum. The complexes were incubated in a 50% (v/v) rat serum solution for various time periods (0 to 24 h). (a) Gel images. (b) Relative

intensity graph of bands. The error bars in the graph represent standard deviations (n = 3).

There are various types of PEI-based siRNA delivery platforms that take advantage of its high transfection efficiency *in vitro*. Nevertheless, the potential of PEI has been particularly limited *in vivo* because of its high toxicity and lack of targetability. Accordingly, several attempts have been made to reduce the cytotoxicity of PEI, including use of linear or low molecular weight PEI and conjugation of PEI to polysaccharide or PEG. Even though these approaches reduced the cytotoxicity of PEI, the main drawback was the decrease in transfection efficiency resulting from chemical modification.

To reduce the toxicity of PEI, we chose the lowest weight ratio of PEI to siRNA complexes (0.8:1) that was able to form relatively stable complexes with AuNPs. In addition, PEGylated HA with high biocompatibility was coated on the surface of complexes. The *in vitro* cytotoxic effects of the complexes on cancer cells (B16F10) and normal cells (NIH3T3) were evaluated using the MTT colorimetric assay (Fig. S2). In CD44-overexpressing B16F10 cells, GDCs resulted in cytotoxicity at high concentrations (>25 μg/ml). In contrast, GICs exhibited only slight toxicity, even at high concentrations (50 μg/ml). Godbey et al. reported that the process of PEI-mediated cell transfection mainly results in two types of cytotoxicity.[31] One is an immediate toxicity of free PEI, while the other is a delayed toxicity upon cellular processing of the PEI/DNA complexes.[32] Interestingly, both GDCs and GICs showed negligible toxicity in CD44-deficient NIH3T3 cells at concentrations of up to 50 μg/ml (Fig. S2b). These results indicate that cytotoxicity is affected by the expression level of CD44 on cells and that the unique structure of GICs with reduced amino groups results in reduced toxicity.

The cellular uptake behavior of complexes was evaluated with different cell types. To detect fluorescent signals, complexes were formed with YOYO-1-labeled siRNA. Afterwards, the complexes were incubated with B16F10 and NIH3T3 cells, and their cellular uptake behaviour was visualized using a confocal microscope. For the CD44-overexpressing B16F10 cancer cells, strong green fluorescent signals were observed when they were treated with GDCs and GICs, whereas no detectable signals were found for the CD44-deficient NIH3T3 cells (Fig. S3a). The quantitative analysis using flow cytometry indicated that, compared to free siRNA, GDCs and GICs exhibited 2.3-fold and 3.0-fold higher uptake by B16F10 cells, respectively (Figs. S3b and c). The cellular distribution of complexes was also observed by labelling endosomes/lysosomes with LysoTracker Red (Fig. S4).[33] The confocal images indicate that green fluorescence (YoYo-1 siRNA) are partially distributed in stained endo-lysosomes, which treated both GDCs and GICs. These results indicate that cellular uptake of complexes occurs through the HA receptor, CD44.

The gene silencing effects of complexes were examined using RFP-expressing cells (Fig. S5). After treatment with the GDCs and GICs (siRNA concentration 200 nM), the red fluorescence signal from RFP-B16F10 cells was considerably reduced, in contrast to the signal from cells treated with the control or free siRNA. This high transfection efficiency might be due to the effective cellular uptake of complexes through receptor-mediated endocytosis and also to efficient intracellular release of siRNAs.

While various siRNA complex systems have been demonstrated to be effective *in vitro*, these results are frequently only a poor reflection of the *in vivo* situation. Therefore, it is critical to examine the fate of the complexes *in vivo*. To investigate the *in vivo* biodistribution and tumor targeting characteristics of complexes, Cy5.5-labeled complexes were administered into the tail veins of SCC7 tumor-bearing mice and the NIRF images were monitored as a function of time. As shown in Fig. 3a, considerable fluorescence signal was detected from complexes one hour after injection. The strongest signals were observed at tumor sites for both GDCs and GICs as a function of time. This might be attributed to the PEGylated HA surface of the complexes that allows for its specific binding to CD44 on tumor cells. Interestingly, for the GICs, the fluorescence signal at the tumor site increased steadily over the initial 6 h. Moreover, signals from the GICs were always stronger than those from the GDCs, implying that the GICs effectively accumulated at the tumor site. Fig. 3b shows a quantitative analysis of the fluorescence intensity at the tumor site over time. *Ex vivo* images of fluorescence distribution within the major organs indicates that the GICs exhibited high tumor accumulation and slow excretion, compared to the GDCs (Fig. 3c). The fluorescence signal from the GICs in tumor was 1.9-fold stronger than the signal from the GDCs (Fig. 3d). Overall, these results suggest that improving the stability of complexes has a great influence on their tumor targetability *in vivo*.

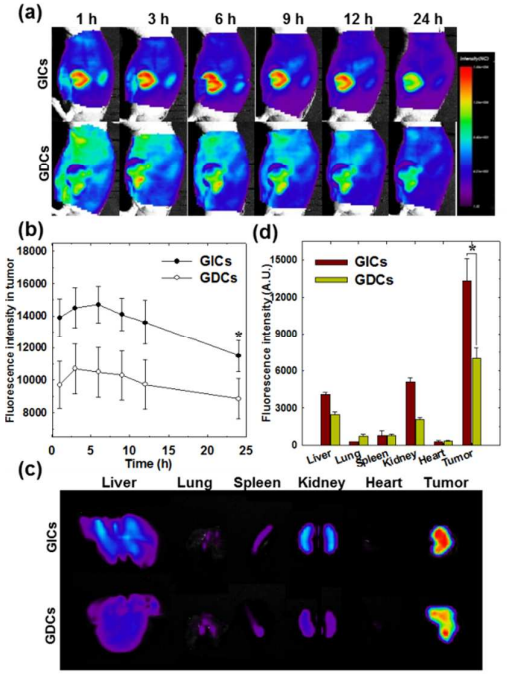

Fig. 3 *In vivo* biodistribution of GDCs and GICs in SCC7 tumor-bearing mice. (a) Whole body images of the mice. (b) Fluorescence intensity at the tumor site as function of time. *Ex vivo* fluorescence images of GDCs and GICs in SCC7 tumor-bearing mice. (c) NIR images of the organs and tumors. (d) Fluorescence intensity of the organs. The error bars in the graph represent standard deviation (n = 3).

For further assessment, the *in vivo* gene silencing efficacies of complexes were evaluated using RFP-B16F10 tumor-bearing mice. After measurement of the red fluorescence signals of mice at the tumor site (0 day) and saline solution as the control, the complexes (10 μg of siRNA/mouse) were injected daily for 3 days into the mice. By comparing the fluorescence images obtained on days 0 and 3, the gene silencing effects of the complexes were estimated (Fig. 4a). The RFP signal intensity at the tumor site after 3 days declined significantly for the GDCs and GICs-treated mice, whereas enhanced fluorescence signals were observed at the tumor site for mice treated with saline, free siRNA and scrambled GICs. As expected, the lowest fluorescence signals were detected in the GIC-treated mice. The relative fluorescence intensity of the tumor region of interest (ROI) is presented in Fig. 4b. For the complexes, fluorescence intensity fell below the zero point, which was established as the fluorescence intensity on the initial day, while the fluorescence intensity increased for the saline and free siRNA. Overall, these results demonstrate that the GICs possess excellent gene silencing ability *in vivo*, mainly thanks to their high stability and tumor targetability.

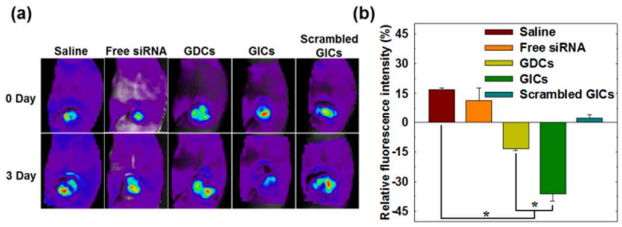

Fig. 4 *In vivo* gene silencing effect of the saline, free siRNA, GDCs, GICs and scrambled GICs in RFP-B16F10 tumor-bearing mice. (a) Whole body images of the mice. (b) Relative fluorescence intensity of tumor ROI. The error bars in the graph represent standard deviation (n = 3).

GICs were prepared and used as carriers for efficient delivery of siRNA. Owing to the presence of AuNPs, the GICs showed outstanding stability compared with the GDCs or free siRNA in the presence of serum. Furthermore, the GICs were able to effectively internalize into the target cells through receptor-mediated endocytosis and release siRNA into the cytosol. As a result, the GICs exhibited high tumor targetability and excellent *in vivo* gene silencing efficiency. Overall, these results suggest that the GIC complexes could potentially be applied as a siRNA carrier for tumor-targeted therapy.

This work was financially supported by the Korea Healthcare Technology R&D Project (HI14C03810200) and the National R&D Program for Cancer Control (1420040) of MHW, and the Global Research Laboratory Program (NRF-2013K1A1A2A02076442) and the Basic Science Research Programs (20100027955 & 2015R1A2A2A05001390) of NRF.

Notes and references

1 S. M. Elbashir, J. Harborth, W. Lendeckel, A. Yalcin, K. Weber and T. Tuschl, *Nature*, 2001, **411**, 494-498.
2 D. Bumcrot, M. Manoharan, V. Koteliansky and D. W. Sah, *Nat. Chem. Biol.*, 2006, **2**, 711-719.
3 D. H. Kim and J. J. Rossi, *Nat. Rev. Genet.*, 2007, **8**, 173-184.
4 M. P. Czech, M. Aouadi and G. J. Tesz, *Nat. Rev. Endocrinol.*, 2011, **7**, 473-484.
5 B. L. Davidson and P. B. McCray, *Nat. Rev. Genet.*, 2011, **12**, 329-340.
6 D. Reischl and A. Zimmer, *Nanomedicine: Nanotechnol. Biol. Medicine*, 2009, **5**, 8-20.
7 Y. Zhou, C. Zhang and W. Liang, *J. Controlled Release*, 2014.
8 M. R. Lares, J. J. Rossi and D. L. Ouellet, *Trends Biotechnol.*, 2010, **28**, 570-579.
9 B. Ozpolat, A. K. Sood and G. Lopez-Berestein, *Adv. Drug Delivery Rev.*, 2014, **66**, 110-116.
10 A. Elbakry, A. Zaky, R. Liebl, R. Rachel, A. Goepferich and M. Breunig, *Nano Lett.*, 2009, **9**, 2059-2064.
11 D. A. Giljohann, D. S. Seferos, A. E. Prigodich, P. C. Patel and C. A. Mirkin, *J. Am. Chem. Soc.*, 2009, **131**, 2072-2073.
12 S. Matsumoto, R. J. Christie, N. Nishiyama, K. Miyata, A. Ishii, M. Oba, H. Koyama, Y. Yamasaki and K. Kataoka, *Biomacromolecules*, 2008, **10**, 119-127.
13 H. Y. Yoon, H. R. Kim, G. Saravanakumar, R. Heo, S. Y. Chae, W. Um, K. Kim, I. C. Kwon, J. Y. Lee and D. S. Lee, *J. Controlled Release*, 2013, **172**, 653-661.
14 P. Ghosh, G. Han, M. De, C. K. Kim and V. M. Rotello, *Adv. Drug Delivery Rev.*, 2008, **60**, 1307-1315.
15 D. A. Giljohann, D. S. Seferos, W. L. Daniel, M. D. Massich, P. C. Patel and C. A. Mirkin, *Angew. Chem. Int. Ed.*, 2010, **49**, 3280-3294.
16 G. B. Braun, A. Pallaoro, G. Wu, D. Missirlis, J. A. Zasadzinski, M. Tirrell and N. O. Reich, *Acs Nano*, 2009, **3**, 2007-2015.
17 J. Entwistle, C. L. Hall and E. A. Turley, *J. Cell. Biochem.*, 1996, **61**, 569-577.
18 T. C. Laurent, *Acta Oto-Laryngol.*, 1987, **104**, 7-24.
19 L. Lapčík, L. Lapcik, S. De Smedt, J. Demeester and P. Chabrecek, *Chem. Rev.*, 1998, **98**, 2663-2684.
20 B. P. Toole, *Nat. Rev. Cancer*, 2004, **4**, 528-539.
21 R. Stern and M. J. Jedrzejas, *Chem. Rev.*, 2006, **106**, 818-839.
22 B. Zhou, J. A. Weigel, L. Fauss and P. H. Weigel, *J. Biol. Chem.*, 2000, **275**, 37733-37741.
23 K. Y. Choi, K. H. Min, H. Y. Yoon, K. Kim, J. H. Park, I. C. Kwon, K. Choi and S. Y. Jeong, *Biomaterials*, 2011, **32**, 1880-1889.
24 K. Y. Choi, H. Y. Yoon, J.-H. Kim, S. M. Bae, R.-W. Park, Y. M. Kang, I.-S. Kim, I. C. Kwon, K. Choi and S. Y. Jeong, *Acs Nano*, 2011, **5**, 8591-8599.
25 P.-L. Kuo, C.-C. Chen and M.-W. Jao, *J. Phys. Chem. B*, 2005, **109**, 9445-9450.
26 J. Newman and G. Blanchard, *Langmuir*, 2006, **22**, 5882-5887.
27 J. Newman and G. Blanchard, *J. Nanopart. Res.*, 2007, **9**, 861-868.
28 I. Moret, J. Esteban Peris, V. M. Guillem, M. Benet, F. Revert, F. Dasí, A. Crespo and S. F. Aliño, *J. Controlled Release*, 2001, **76**, 169-181.
29 M. H. Stewart, K. Susumu, B. C. Mei, I. L. Medintz, J. B. Delehanty, J. B. Blanco-Canosa, P. E. Dawson and H. Mattoussi, *J. Am. Chem. Soc.*, 2010, **132**, 9804-9813.
30 F. Alexis, E. Pridgen, L. K. Molnar and O. C. Farokhzad, *Mol. Pharm.*, 2008, **5**, 505-515.
31 W. Godbey, K. K. Wu and A. G. Mikos, *Biomaterials*, 2001, **22**, 471-480.
32 D. Fischer, Y. Li, B. Ahlemeyer, J. Krieglstein and T. Kissel, *Biomaterials*, 2003, **24**, 1121-1131.
33 R. Sheng, F. An, Z. Wang, M. Li and A. Cao, *RSC Adv.*, 2015, **5**, 12338-12345.